Nanoscale structures of radiation-grafted polymer electrolyte membranes investigated via a small-angr,ru neutron scattering technique

by Ananda Putra

ORIGINAL ARTICLE

Nanoscale structures of radiation-grafted polymer electrolyte membranes investigated via a small-angle neutron scattering technique

Shin-ichi Sawada[1], Daisuke Yamaguchi[2], Ananda Putra[2], Satoshi Koizumi[3] and Yasunari Maekawa[1]

The nanoscale structures of graft-type polymer electrolyte membranes (PEMs), prepared by radiation-induced graft polymerization (grafting) of styrene onto poly(ethylene-*co*-tetrafluoroethylene) (ETFE) films followed by sulfonation, were investigated using a small-angle neutron scattering (SANS) technique. For comparison, SANS measurements were also performed on two precursor materials, the original ETFE film and polystyrene (PS)-grafted films. The SANS profiles of the grafted films showed shoulder peaks at a d-spacing of $\sim 30\,nm$, which were attributed to the PS grafts introduced into the amorphous phases between the ETFE lamellar crystals. This grafting would result in the construction of a stack structure with alternating ETFE crystalline and PS-grafted layers as a repeating unit. In the ETFE PEMs, the spacing of the PS sulfonic acid (PSSA) grafts and ETFE crystals increased because the graft regions were enlarged by the volume of the attached sulfonic acid groups. Interestingly, the graft/crystal stack spacing in the PEMs did not increase from the dry- to fully-hydrated states. This finding implies restricted water absorption in the PSSA grafts between the ETFE lamellar crystals. In other words, most of the PSSA grafts introduced outside of the lamellae were considered to be hydrated and to act as proton conduction pathways.
Polymer Journal (2013) 45, 797–801; doi:10.1038/pj.2012.218; published online 12 December 2012

Keywords: polymer electrolyte membranes; radiation grafting; small-angle neutron scattering

INTRODUCTION

Polymer electrolyte membrane (PEM) fuel cells are expected to be next-generation environmentally friendly energy conversion devices.[1,2] PEMs are vital components in PEM fuel cells, because their properties significantly influence cell performance. At present, the most commonly used PEM is Nafion (DuPont Co., Wilmington, DE, USA), which possesses high chemical stability and mechanical strength. However, the proton conductivity of Nafion dramatically drop above 100 °C, which prevents Nafion from being employed in practical fuel cell systems. Moreover, the production of Nafion is expensive owing to the complicated fluorine chemical process. These drawbacks have stimulated the development of alternative PEM materials worldwide.

In recent years, radiation-induced graft polymerization has become a promising new technique for synthesizing fuel cell PEMs.[3,4] This technique involves irradiation of base fluoropolymer films, grafting of styrene or styrene-derivative monomers into the irradiated base films, and sulfonation of the aromatic rings in the graft chains. The fluoropolymers commonly used as base films include polytetrafluoroethylene (PTFE), poly(tetrafluoroethylene-*co*-hexafluoroethylene) (FEP), poly[tetrafluoroethylene-*co*-perfluoro (propyl vinyl ether)] (PFA), poly(ethylene-*co*-tetrafluoeoethylene)

(ETFE), and poly(vinylidene fluoride). One of the main advantages of this radiation grafting method is the control of the ion exchange capacity (IEC) of PEMs over a wide range up to 3.0 meq g^{-1}, which is far greater than that of Nafion (0.90 meq g^{-1}).

The morphological structure of PEMs is one of the main concerns not only with respect to fundamental research but also for the development of high-performance fuel cells. In PEMs, the fixed sulfonic acid groups and absorbed water are considered to form hydrophilic domains that are phase-separated from the hydrophobic polymer backbones. Such a phase-separation morphology should affect various PEM properties such as proton conductivity, chemical stability and mechanical strength. Over the past few decades, a considerable number of studies have been performed on Nafion, and several structural models have been proposed.[5] According to the most popular model (Gierke's model), spherical hydrophilic domains with a diameter of 3–5 nm are embedded in the hydrophobic PTFE matrices.[6] However, for the graft-type PEMs, there have been only a few studies that have revealed structural information.

In the present study, the nanoscale structures of ETFE-based graft-type PEMs were investigated using a small-angle neutron scattering (SANS) technique. These PEMs were composed of crystalline and amorphous phases of ETFE, and the introduced graft regions.

[1]High Performance Polymer Group, Quantum Beam Science Directorate, Japan Atomic Energy Agency, Gunma, Japan; [2]Strongly Correlated Supramolecules Group, Quantum Beam Science Directorate, Japan Atomic Energy Agency, Ibaraki, Japan and [3]College of Engineering, Ibaraki University, Ibaraki, Japan
Correspondence: Dr S Sawada, Quantum Beam Science Directorate, Japan Atomic Energy Agency, 1233 Watanuki, Takasaki, Gunma 370-1292, Japan.
E-mail: sawada.shinnichi@jaea.go.jp

Accordingly, the precursor base ETFE and polystyrene (PS)-grafted films were also subjected to SANS measurements as references. Comparisons of the results for the ETFE, PS-grafted films and PEMs enabled us to probe the crystal morphology. Balog *et al.*[7] also performed SANS measurement on ETFE-based graft-type PEMs, in which the graft chains were crosslinked with divinylbenzene. They focused on the effect of the divinylbenzene crosslink level on the structures of PEMs possessing a narrow range of IECs. In contrast, in this study, PEMs with various IECs were measured to examine the IEC dependence of the morphological structures. In addition, the SANS profiles were more carefully analyzed to gather more detailed information about the structure, for example, the locations where the grafts were introduced in the base ETFE film.

EXPERIMENTAL PROCEDURE
Synthesis of PEMs
ETFE films (Asahi Grass Co., Tokyo, Japan) with a thickness of 50 μm as the base fluoropolymer were irradiated at room temperature using 15 kGy γ-rays in glass ampoules filled with Ar. For the grafting, the irradiated films were immediately immersed in a styrene monomer solution, and then kept at 60 °C for 4–6 h. After the grafting reaction, the films were washed with toluene to remove any excess styrene monomers. The grafted films were then dried under vacuum at 40 °C to a constant weight. The degree of grafting (DOG) was estimated using the following equation:

$$DOG = \frac{W_G - W_O}{W_O} \times 100 \qquad (1)$$

where W_O and W_G are the weights of the base ETFE and grafted films, respectively. The DOG for the three prepared grafted films was 16, 31 and 58%.

For sulfonation, the PS-grafted films were immersed in a 0.2 M chlorosulfonic acid/1,2-dichloroethane mixture at 50 °C for 6 h. Finally, the resulting PEM was rinsed with pure water and then dried under vacuum. The IEC of the PEM was measured by acid-base back titration with a standardized 0.1 M NaOH solution. The three prepared PEMs possessed IECs of 1.1, 1.8 and 2.7 meq g^{-1}, which corresponds to DOGs of 16, 31 and 58%, respectively. Here, the expected values of the IEC were calculated from the DOG on the basis of the assumption that sulfonic acid groups are attached to all the aromatic rings of the grafted styrene units. The ratio of the measured to expected IEC was over 90% for all three PEMs.

SANS measurement
SANS measurements were performed using a focusing and polarized SANS spectrometer (SANS-J-II) at the JRR-3 research reactor at the Japan Atomic Energy Agency (JAEA) in Tokai, Japan. The film and PEM samples were held in quartz cells at 25 °C during the entire experiment. The wavelength of the incident neutron was 0.65 nm with a wavelength resolution of 13%. The SANS profiles were obtained with sample-to-detector distances of 10 and 2.5 m, corresponding to a scattering vector magnitude, *q*, of 0.04–1 nm^{-1}. The scattering profiles were detected with a two-dimensional position sensitive detector. The measured two-dimensional scattering patterns were circular-averaged, and then the absolute intensity per sample volume, *I(q)*, was obtained.

RESULTS AND DISCUSSION
Original ETFE film, PS-grafted film and PEM
The SANS intensity of the original ETFE film was too weak to provide us with any meaningful information. Thus, to examine the structure of the ETFE film, small-angle X-ray scattering (SAXS) analysis was performed (Figure 1). A sharp peak was observed at the *q* of 0.30 nm^{-1}, corresponding to a real correlation distance, *d* (= 2π/ *q*), of 21 nm. This *d* value was assumed to be the lamellar spacing, that is, the intervals between the ETFE crystalline layers. This value is in good agreement with the previously reported value of *q* (= 0.24 nm^{-1}; *d* = 26 nm) corresponding to the lamellar structures,
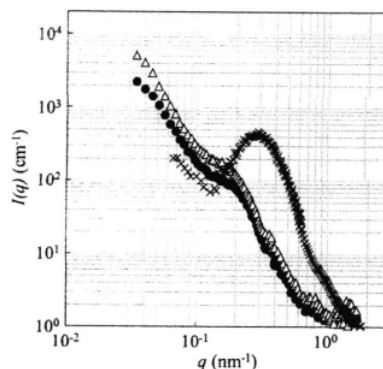

Figure 1 Small-angle neutron scattering (SANS) profiles of a (●) grafted film (degree of grafting (DOG) = 31%) and (Δ) polymer electrolyte membrane (PEM) (ion exchange capacity (IEC) = 1.8 meq g^{-1}) in the dried state. For comparison, this figure shows the SAXS profile (×) of the base poly(ethylene-*co*-tetrafluoethylene) (ETFE) film.

which was obtained for the SAXS measurement of an ETFE film.[8] The much lower SANS intensity compared with the SAXS intensity was owing to the small difference in the neutron scattering length density between the ETFE amorphous and crystalline phases.

Figure 1 also shows the representative SANS profiles of a grafted film (DOG = 31%) and PEMs (IEC = 1.8 meq g^{-1}) in the dried state. The SANS intensity of these samples was far greater than that of the base ETFE film, reflecting the significant difference in the neutron scattering length density between the PS or poly(styrene sulfonic acid) (PSSA) graft regions and ETFE matrices. For the grafted film, a shoulder-like peak appeared at *q* = 0.21 nm^{-1}, which corresponds to a *d* of 30 nm. This result suggests that the PS-graft regions existed at regular spatial intervals of 30 nm. In previous SANS measurements of the FEP- and ETFE-based PS-grafted films,[7,9] this peak was also observed at a similar *q*. However, the interpretation of this peak was not so clear in these studies.[7,9] Thus, the ordered structures responsible for the observed peak in the PS-grafted film were considered.

First, an understanding of the radiation grafting process onto base polymer films is necessary. Ionizing radiation such as γ-ray and electron beam homogeneously produces free radicals in base polymer films. The radicals in the amorphous phases are considered to quickly vanish because of recombination and disproportionation reactions between two radicals, whereas the radicals can survive in the crystalline phases, where polymer chain motion is strongly restricted. When the radicals in the crystalline phases migrate to the crystalline/amorphous boundaries, they encounter monomers that can diffuse only in the amorphous phases, resulting in the initiation of graft polymerization. The graft chains are then elongated into the amorphous phases because the monomers cannot easily permeate into the crystalline phases. This grafting kinetics was experimentally confirmed by an electron spin resonance method,[10,11] a X-ray diffraction method[12] and a time-resolved SANS method.[13]

In view of the above facts, attention should be paid to the styrene grafting occuring in the crystalline/amorphous lamellar structures of the ETFE film. Unlike the crystallites, which are impermeable to styrene monomers, the amorphous phases were grafted. The PS-graft chains presumably gathered together and excluded the amorphous ETFE chains owing to the immiscibility of PS and ETFE. This
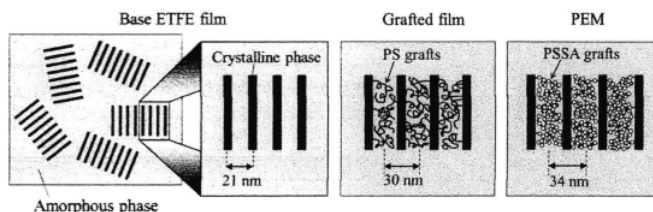
Base ETFE film | Grafted film | PEM

Figure 2 Schematic pictures of the base poly(ethylene-*co*-tetrafluoeoethylene) (ETFE) film, PS-grafted film (degree of grafting (DOG) = 31%), and polymer electrolyte membrane (PEM) (ion exchange capacity (IEC) = 1.8 meq g^{-1}).

immiscibility likely resulted in the formation of alternating stack structures of ETFE crystalline and PS-grafted layers as a repeating unit. Accordingly, we regarded the stacks of the PS-graft regions as the origin of the SANS peak at a q of 0.21 nm^{-1} (d = 30 nm). It is noteworthy that the spatial interval of these graft layers (30 nm) was greater than the spacing of the original ETFE crystalline layers (21 nm). This widening of the lamellar spacing by 1.5 times is likely the result of the presence of the elongated PS-graft chains, which pushed away the crystalline layers. The crystalline/amorphous lamellar structure of the original ETFE film and the PS-graft regions formed between the lamellar crystallites are schematically depicted in Figure 2.

The SANS profile of the PEM also exhibited a shoulder peak at q = 0.18 nm^{-1} (d = 34 nm). This d value was somewhat larger than that for the PS-grafted film (d = 30 nm), indicating an increase in the graft stack spacing as shown in Figure 2. This increase was likely caused by the expansion of the graft regions owing to the greater volume of the attached sulfonic acid groups. Besides, because of the chemical repulsion between the ETFE and PSSA chains (the former and latter are hydrophobic and hydrophilic, respectively), they may try to move away from each other, thereby extending the graft stack spacing.

Grafted films and PEMs with different graft contents
Figure 3a shows the SANS profiles of the grafted films with different DOGs (16−58%). All SANS profiles had shoulder-like peaks at a q of ∼0.2 nm^{-1}. The q value at the peak, q_P, was then converted to the real correlation distance, d_P (= $2\pi/q_P$), which is plotted in Figure 4. For the grafted films, d_P increased from 21 to 33 nm when the DOG increased from 0 to 58%. The increases in d_P with the DOG indicated that substantial amounts of PS grafts were introduced between the ETFE lamellar crystals, thus increasing the graft stack spacing.

As shown in Figure 3a, the PS-grafted films with larger DOGs exhibited a higher $I(q)$ when $q < q_P$, that is, at a larger-scale range than the graft/crystal stack spacing, d_P. This result indicated a structural change in the PS-graft regions, not in the limited area between the lamellar crystals but in the other amorphous areas in the ETFE film. As the PS-graft regions were significantly expanded with the DOG, the difference in scattering length density between the PS grafts and ETFE matrices became more pronounced, resulting in the enhanced $I(q)$. On the other hand, at $q > q_P$, $I(q)$ was nearly the same regardless of the DOG (Figure 3a). In these grafted films, PS-filled graft regions are probably formed even at the smallest DOG of 16%, which would account for the independence of $I(q)$ on the DOG in the range of 16–58%. In Figure 3a, it can be also seen that the plots for all grafted films at $q > q_P$ obey Porod's law with a q^{-4} decay, which characterizes a two-phase system with a sharp boundary.[14] This result suggests that
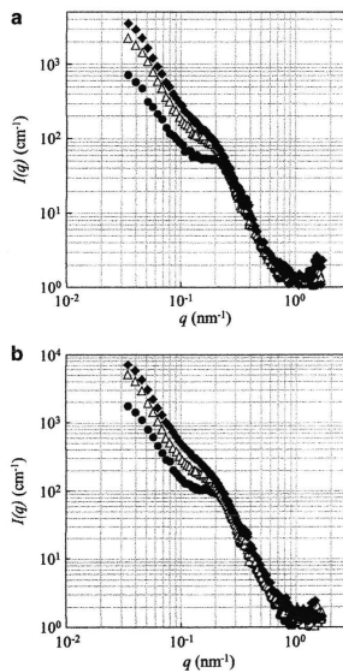

Figure 3 Small-angle neutron scattering (SANS) profiles of (**a**) the grafted films with different degrees of grafting (DOGs) of (●) 16%, (△) 31%, and (◇) 58%; (**b**) polymer electrolyte membranes (PEMs) with different ion exchange capacity (IECs) of (●) 1.1 meq g^{-1}, (△) 1.8 meq g^{-1}, and (◇) 2.7 meq g^{-1}.

the PS grafts and ETFE matrices were distinctly phase-separated from each other. In addition, in the measured q range 3.4×10^{-2}–1.6 nm^{-1} (d = 180–3.9 nm), there was no other peak but the one attributed to the grafts between the lamellar crystals. Accordingly, it was assumed that the PS-graft regions did not have periodically ordered structures on this spatial scale, but existed as continuous domains with a large size of at least 180 nm. This result is also considered to support the clear phase-separation between the PS grafts and ETFE matrices. In contrast, if the phase-separation had been ambiguous, the graft regions would have been divided by the ETFE chains into a far
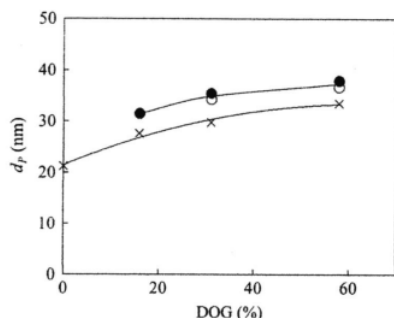
Figure 4 Relationship between d_P and degree of grafting (DOG) for ($\times$) the grafted films and polymer electrolyte membranes (PEMs) in ($\bigcirc$) the dried and ($\bullet$) hydrated states. For the plots of the PEMs, the DOGs of 16, 31 and 58% correspond to the ion exchange capacity (IECs) of 1.1, 1.8 and 2.7 meq g^{-1}, respectively.

smaller size. In Mortensen *et al.*'s work[9] regarding SANS measurements of FEP-based PS-grafted films, the clear phase-separation between the PS-grafted regions and FEP matrices was surmised. In their paper, the peak observed at the small q of 0.035 nm^{-1} ($d = 180$ nm) was assumed to be derived from PS aggregates separated from the FEP backbones. To reveal such larger-scale structures in the grafted films evaluated in our study, SANS measurements in the lower q range are required.

Figure 3b shows the SANS profiles of PEMs with IECs of 1.1–2.7 meq g^{-1} in the dried state. All PEMs exhibited shoulder-like peaks, yielding the d_P values shown in Figure 4. At every DOG, d_P was larger than that for the grafted films. As mentioned above, this increase should be caused by two factors: volume expansion due to the sulfonic acid groups and repulsive interaction between the PSSA and ETFE chains. Similar to the grafted films, $I(q)$ at $q > q_P$ decreased with a q^{-4} power law, indicating clear phase-separation between the PSSA-graft regions and ETFE matrices. This conclusion is quite opposite to Balog's work, in which the PSSA chains were assumed to be mixed with the ETFE chains.[7]

PEMs in the dried and hydrated states

Figure 5 shows the SANS profiles of the PEMs in the dried and hydrated states. The hydrated PEMs also exhibited shoulder-like peaks and the obtained d_P values are shown in Figure 4. It was found that the d_P values for all PEMs were nearly the same in both dried and hydrated states, implying no water absorption in the graft regions between the lamellar crystals. The two experimental facts, that is, that the sulfonation degree was $>90\%$ and that the crystallinity of the ETFE film was 35%, suggest almost full sulfonation of the PS grafts including even those between the lamellar crystals. Accordingly, a possible explanation for no change in d_P by the water absorption is that water did not penetrate into the PSSA-graft regions between the lamellar crystals in spite of their hydrophilic character.

It is accepted that the swelling of water occurs only in the hydrophilic PSSA-graft regions and not in the hydrophobic fluoropolymer parts. In fact, according to a dissipative particle dynamics simulation of graft-type PEMs,[15] absorbed water was found to penetrate into the PSSA graft chains to form mixed domains completely segregated from the fluoropolymer parts. It follows that the PSSA-graft regions in the PEMs in this study were enlarged by the
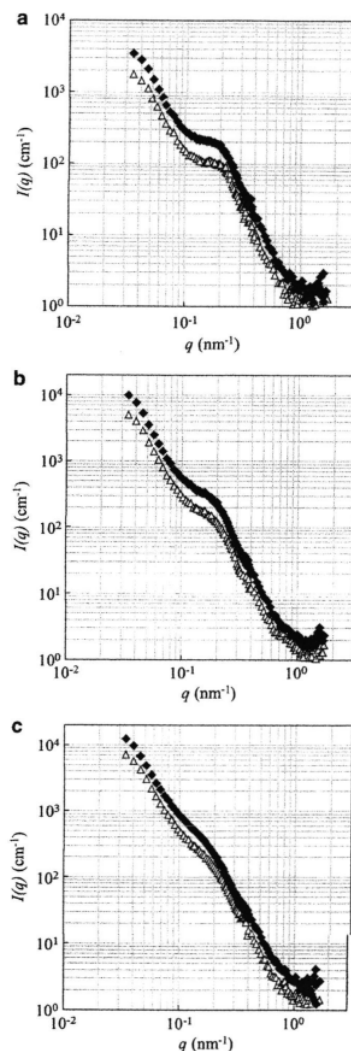
Figure 5 Small-angle neutron scattering (SANS) profiles of the polymer electrolyte membranes (PEMs) with ion exchange capacity (IECs) of (a) 1.1, (b) 1.8 and (c) 2.7 meq g^{-1} in ($\triangle$) the dried and ($\blacklozenge$) hydrated states.

volume of absorbed water. Thus, the volume change ratio of the hydrated to dried graft regions, K, was calculated using the following equation:

$$K = \frac{W_{PSSA}/\rho_{PSSA} + W_{water}/\rho_{water}}{W_{PSSA}/\rho_{PSSA}} \qquad (2)$$

where W_{PSSA} and ρ_{PSSA} are the weight and density (1.46 g cm^{-3}) of the PSSA-graft regions, and W_{water} and ρ_{water} are the weight and density (1.00 g cm^{-3}) of the absorbed water. The value for W_{PSSA} in

Table 1 K and L values of the PEMs

DOG (%)	IEC (meq g^{-1})	K	L
16	1.1	2.22	1.30
31	1.8	2.43	1.34
58	2.7	3.04	1.45

Abbreviations: DOG, degree of grafting; IEC, ion exchange capacity; PEM, polymer electrolyte membrane.

equation (2) was calculated from the DOG as follows:

$$W_{PSSA} = \frac{M_{SSA} \times DOG \times W_O}{100 \times M_{St}} \quad (3)$$

where M_{SSA} and M_{St} are the molecular weights of a styrene sulfonic acid unit (184 g mol^{-1}) and a styrene unit (104 g mol^{-1}), respectively. The value W_{water} in equation (2) was then calculated from the water uptake measurement as follows:

$$W_{water} = W_{PEM, hyd} - W_{PEM, dry} \quad (4)$$

where $W_{PEM, hyd}$ and $W_{PEM, dry}$ are the weights of the PEM samples in the hydrated and dried states, respectively. The K values calculated from equation (2) are listed in Table 1. As the IEC increased from 1.1 to 2.7 meq g^{-1}, K increased from 2.22 to 3.04. Given that the PSSA-graft regions swelled in an isotropic manner, their one-dimensional swelling degree, L, was calculated as follows:

$$L = \sqrt[3]{K} \quad (5)$$

The L values of all PEMs are also listed in Table 1.

If all PSSA-graft regions are enlarged by absorbing water in the same way, the d_P values increase by a factor of L. Contrary to this expectation, as mentioned above, d_P was not changed when the PEMs were hydrated (Figure 4). One possible explanation for this result is that the PSSA-graft regions were sandwiched and suppressed by the ETFE lamellar crystal and could not expand owing to water sorption. That is, water may not be smoothly absorbed in the graft regions between the ETFE lamellar crystals. Such a water-poor environment would significantly slow down proton conduction because protons have to move through the hydrogen-bond network mediated by water molecules. Consequently, the PSSA grafts between the lamellar crystals possibly do not contribute to the proton conductivity of the PEMs.

The $I(q)$ curves at $q > q_P$ were also similar to each other in both dried and hydrated states (Figure 5). On the other hand, when $q < q_P$, $I(q)$ of the hydrated PEMs was somewhat higher than that of the dried PEMs. The SANS data at $q = q_P$ reflects the structures of the PSSA-grafted regions not only between the lamellar crystals but also outside of the crystals. Although water absorption is presumably restricted in the former graft regions, the latter graft regions can absorb water and expand to some extent. Namely, the PSSA graft regions with larger size than the lamellar spacing corresponding to $q = q_P$ increased by the water absorption, resulting in the increases of the $I(q)$ at $q < q_P$. These hydrated graft regions are thus considered to play the role of proton conduction pathways. It is conjectured from the SANS measurements that the crystalline structures of the base polymer films likely influence the proton conduction properties of the graft-type PEMs.

CONCLUSIONS

The nanoscale structures of ETFE-based graft-type PEMs were investigated by the SANS technique. As references, SANS measurements were performed on the precursor base ETFE and PS-grafted films. The SANS profile of a grafted film (DOG = 31%) exhibited a shoulder-like peak at a d of 30 nm, which was assumed to originate from PS-graft stacks located between the ETFE lamellar crystals. In the PEM obtained by sulfonation (IEC = 1.8 meq g^{-1}), the PSSA-graft stack spacing increased to 34 nm because the graft regions were enlarged by the volume of the attached sulfonic acid groups and the repulsive interaction between the PSSA and ETFE chains. As IEC increased, the amount of PSSA grafts introduced between the ETFE lamellae increased, which widened the graft stack spacing. The SANS plots of all PEMs obeyed Porod's law with a q^{-4} decay, indicating a distinct phase-separation between the PSSA grafts and ETFE matrices. Interestingly, the stack spacing of the PSSA grafts was not very different in the dried- and fully-hydrated states, suggesting restricted water sorption. Under such water-poor conditions, the PSSA grafts between the ETFE lamellar crystals may not contribute to proton conduction because protons move through the hydrogen-bond network mediated by water molecules. It was implied from the SANS measurements that the proton conductivity of the graft-type PEMs is related to the crystallite structures in the base polymer films.

1 Smitha, B., Sridhar, S. & Khan, A. A. Solid polymer electrolyte membranes for fuel cell applications—a review. *J. Membr. Sci.* **259**, 10–26 (2005).
2 Wang, Y., Chen, K. S., Mishler, J., Cho, S. C. & Adroher, X. C. A review of polymer electrolyte membrane fuel cells: technology, applications, and needs on fundamental research. *Appl. Energy* **88**, 981–1007 (2011).
3 Nasef, M. M. & Hegazy, E. S. A. Preparation and applications of ion exchange membranes by radiation-induced graft copolymerization of polar monomers onto non-polar films. *Prog. Polym. Sci.* **29**, 499–561 (2004).
4 Gubler, L., Gürsel, S. A. & Scherer, G. G. Radiation grafted membranes for polymer electrolyte fuel cells. *Fuel Cells* **5**, 317–335 (2005).
5 Mauritz, K. A. & Moore, R. B. State of understanding of nafion. *Chem. Rev.* **104**, 4535–4585 (2004).
6 Gierke, T. D., Munn, G. E. & Wilson, F. C. The morphology in nafion perfluorinated membrane products as determined by wide- and small-angle X-ray studies. *J. Polym. Sci. Polym. Phys. Ed.* **19**, 1687–1704 (1981).
7 Balog, S., Gasser, U., Mortensen, K., Gubler, L., Scherer, G. G. & Youcef, H. B. Correlation between morphology, water uptake, and proton conductivity in radiation-grafted proton-exchange membranes. *Macromol. Chem. Phys.* **211**, 635–643 (2010).
8 Funaki, A., Arai, K., Aida, S., Phongtamrug, S. & Tashiro, K. Influence of third monomer on the crystal phase transition behavior of ethylene-tetrafluoroethylene copolymer. *Polymer (Guildf)* **49**, 5497–5503 (2008).
9 Mortensen, K., Gasser, U., Gürsel, S. A. & Scherer, G. G. Structural characterization of radiation-grafted block copolymer films, using SANS technique. *J. Polym. Sci. Part B Polym. Phys.* **46**, 1660–1668 (2008).
10 Seguchi, T. & Tamura, N. Mechanism of decay of alkyl radicals in irradiated polyethylene on exposure to air as studied by electron spin resonance. *J. Phys. Chem.* **77**, 40–44 (1973).
11 Seguchi, T. & Tamura, N. Electron spin resonance studies on radiation graft copolymerization in polyethylene. II. Grafting initiated by allyl radicals trapped in irradiated polyethylene. *J. Polym. Sci. Polym. Chem. Ed.* **12**, 1953–1964 (1974).
12 Smit, I. & Bezjak, A. Structural changes in the grafted copolymer polyethylene-styrene. *Polymer (Guildf)* **22**, 590–596 (1981).
13 Iwase, H., Sawada, S., Yamaki, T., Maekawa, Y. & Koizumi, S. Preirradiation graft polymerization of styrene in a poly(tetrafluoroethylene) film investigated by time-resolved small-angle neutron scattering. *Int. J. Polym. Sci.* **2011**, doi:10.1155/2011/301807.
14 Roe, R. J. *Methods of X-ray and Neutron Scattering in Polymer Science* ch. 5 176–184 (Oxford University Press, New York, 2000).
15 Sawada, S., Yamaki, T., Ozawa, T., Suzuki, A., Terai, T. & Maekawa, Y. Structural analysis of radiation-grafted polymer electrolyte membranes by dissipative particle dynamics simulation. *Kobunshi Ronbunshu (in Japanese)* **67**, 224–227 (2010).

Nanoscale structures of radiation-grafted polymer electrolyte membranes investigated via a small-angr,ru neutron scattering technique

9%
SIMILARITY INDEX

2%
INTERNET SOURCES

9%
PUBLICATIONS

0%
STUDENT PAPERS

2%

★ Sawada, S.. "Solid polymer electrolyte water electrolysis systems for hydrogen production based on our newly developed membranes, Part I: Analysis of voltage-current characteristics", Progress in Nuclear Energy, 200803
Publication

Exclude quotes	Off	
Exclude bibliography	Off	

Exclude matches	Off